Combining Multinuclear High-Resolution Solid-State MAS NMR and Computational Methods for Resonance Assignment of Glutathione Tripeptide

ARTICLE *in* THE JOURNAL OF PHYSICAL CHEMISTRY A · MAY 2012

Impact Factor: 2.69 · DOI: 10.1021/jp302128r · Source: PubMed

6 AUTHORS, INCLUDING:

Mariana Sardo
University of Aveiro
28 PUBLICATIONS **175** CITATIONS
SEE PROFILE

Joao Rocha
University of Aveiro
455 PUBLICATIONS **9,801** CITATIONS
SEE PROFILE

José R B Gomes
University of Aveiro
188 PUBLICATIONS **2,561** CITATIONS
SEE PROFILE

Luís Mafra
University of Aveiro
86 PUBLICATIONS **1,254** CITATIONS
SEE PROFILE

THE JOURNAL OF PHYSICAL CHEMISTRY A

Article

pubs.acs.org/JPCA

Combining Multinuclear High-Resolution Solid-State MAS NMR and Computational Methods for Resonance Assignment of Glutathione Tripeptide

Mariana Sardo,[†] Renée Siegel,[†] Sérgio M. Santos,[†] João Rocha,[†] José R. B. Gomes,[†] and Luis Mafra*[,†,‡]

[†]Department of Chemistry, CICECO, University of Aveiro, P-3810-193 Aveiro, Portugal

[‡]Departamentos de Química Física y Analítica y Química Orgánica e Inorgánica, Universidad de Oviedo, 33006 Oviedo, Spain

Supporting Information

ABSTRACT: We present a complete set of experimental approaches for the NMR assignment of powdered tripeptide glutathione at natural isotopic abundance, based on *J*-coupling and dipolar NMR techniques combined with ^{1}H CRAMPS decoupling. To fully assign the spectra, two-dimensional (2D) high-resolution methods, such as ^{1}H−^{13}C INEPT-HSQC/PRESTO heteronuclear correlations (HETCOR), ^{1}H−^{1}H double-quantum (DQ), and ^{1}H−^{14}N *D*-HMQC correlation experiments, have been used. To support the interpretation of the experimental data, periodic density functional theory calculations together with the GIPAW approach have been used to calculate the ^{1}H and ^{13}C chemical shifts. It is found that the shifts calculated with two popular plane wave codes (CASTEP and Quantum ESPRESSO) are in excellent agreement with the experimental results.

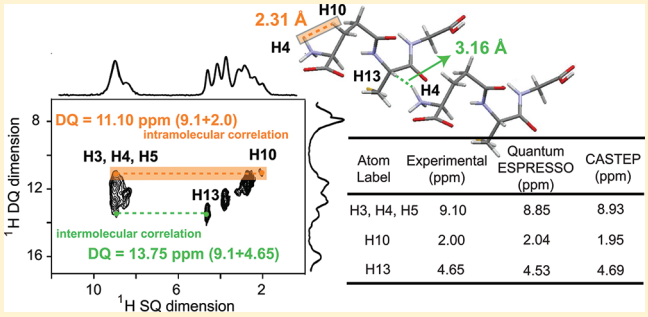

Atom Label	Experimental (ppm)	Quantum ESPRESSO (ppm)	CASTEP (ppm)
H3, H4, H5	9.10	8.85	8.93
H10	2.00	2.04	1.95
H13	4.65	4.53	4.69

INTRODUCTION

Solid-state NMR is a valuable source of structural information, mainly due to the sensitivity of chemical shifts to the structure of molecular crystals.[1] Chemical shifts are widely used as a crystallographic tool, together with other experimental and computational techniques, for both organic and inorganic systems.[1,2] In particular, ^{1}H NMR chemical shifts are a powerful probe for intermolecular interactions, more specifically hydrogen bonding and $\pi\cdots\pi$ interactions, which control the self-assembly of molecules in the solid state. Furthermore, due to the high natural abundance of ^{1}H isotopes, proton NMR is a very sensitive source of chemical information for small molecules.

Small molecules may, at times, be more challenging to the NMR spectroscopist than macromolecules. For instance, biomacromolecules have a wide range of sophisticated isotopic labeling schemes available to facilitate spectral assignment and geometry measurements and may often be treated without considering the crystalline environment. To help in resonance assignment, ab initio codes based on periodic boundary conditions have been widely used regarding the study of small molecules. Prominent examples are available in the literature mostly employing the GIPAW (gauge including projector augmented wave)[3] implemented in the DFT (density functional theory)-based CASTEP commercial code.[4] Several applications of this code have been reported to calculate ^{1}H and ^{13}C chemical shifts of β-maltose[5] and penicillin G[6] molecular systems combining a toolbox of two-dimensional (2D) high-resolution ^{1}H NMR-based methods such as double-quantum (DQ) spectroscopy and *J*-coupling based methods. Other reports are also available on the use of the GIPAW approach to quantify weak crystal packing interactions in small molecules such as uracil, 4-cyano-4′-ethynylbiphenyl,[7] and pharmaceutical systems such as γ-indomethacin[8] and ciprofloxacin.[9]

In contrast, the GIPAW module contained in the open source Quantum ESPRESSO[10] (QE) code may also be used to calculate chemical shifts with good accuracy.[11,12] QE is an integrated suite of computer codes for electronic structure calculations and materials modeling at the nanoscale. It is based on DFT, plane waves, and pseudopotentials (both norm-conserving and ultrasoft). To the best of our knowledge, only three publications presenting chemical shift calculations for indomethacin,[11] polycyclic aromatic hydrocarbons,[12] and several small molecules as well as a copper−phosphine metallocene[13] have been reported. Very recently, a review article by T. Charpentier on the application of the PAW/GIPAW approach for computing NMR parameters has also been published.[14] The small number of contributions using QE in NMR applications may indicate that this code is not yet thoroughly exploited in the field. In this contribution, we compare the GIPAW module packaged with QE and the well-established GIPAW/DFT CASTEP code to better ascertain the potential of the former using the model compound glutathione (GSH). GSH (Figure 1) is a tripeptide

Received: March 5, 2012
Revised: May 18, 2012
Published: May 21, 2012

   dx.doi.org/10.1021/jp302128r | *J. Phys. Chem. A* 2012, 116, 6711−6719

composed of glutamate, cysteine, and glycine (γ-L-glutamyl-L-cysteinyl-glycine) and is the most abundant low-molecular-weight antioxidant synthesized in cells,[15] playing a vital role in the celular oxidative stress.[16]

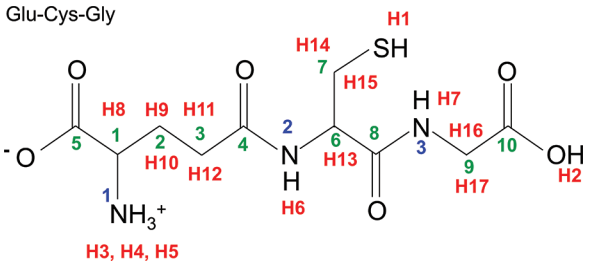

Figure 1. Molecular structure of glutathione (GSH) with atom labels included (carbons in green, protons in red, and nitrogens in blue).

The ethos of this article is to demonstrate the potential of combining a set of multinuclear solid-state NMR methods and computer simulations by means of a specific application to GSH. High-resolution 2D $^{1}H-^{1}H$ DQ-CRAMPS NMR in tandem with 2D $^{1}H-^{14}N$ *D*-HMQC and $^{1}H-^{13}C$ HETCOR (INEPT-HSQC and PRESTO combined with ^{1}H CRAMPS decoupling) NMR experiments are combined to fully assign the spectra of GSH. Our results also reinforce the results obtained by other authors,[11−13] indicating that QE performs, at least, as well as the commercial codes for the determination of theoretical ^{1}H and ^{13}C chemical shifts.

METHODS

CASTEP Calculations. The calculation of NMR chemical shifts was performed within the framework of DFT, using the plane wave pseudopotential formalism and the PBE functional,[17]

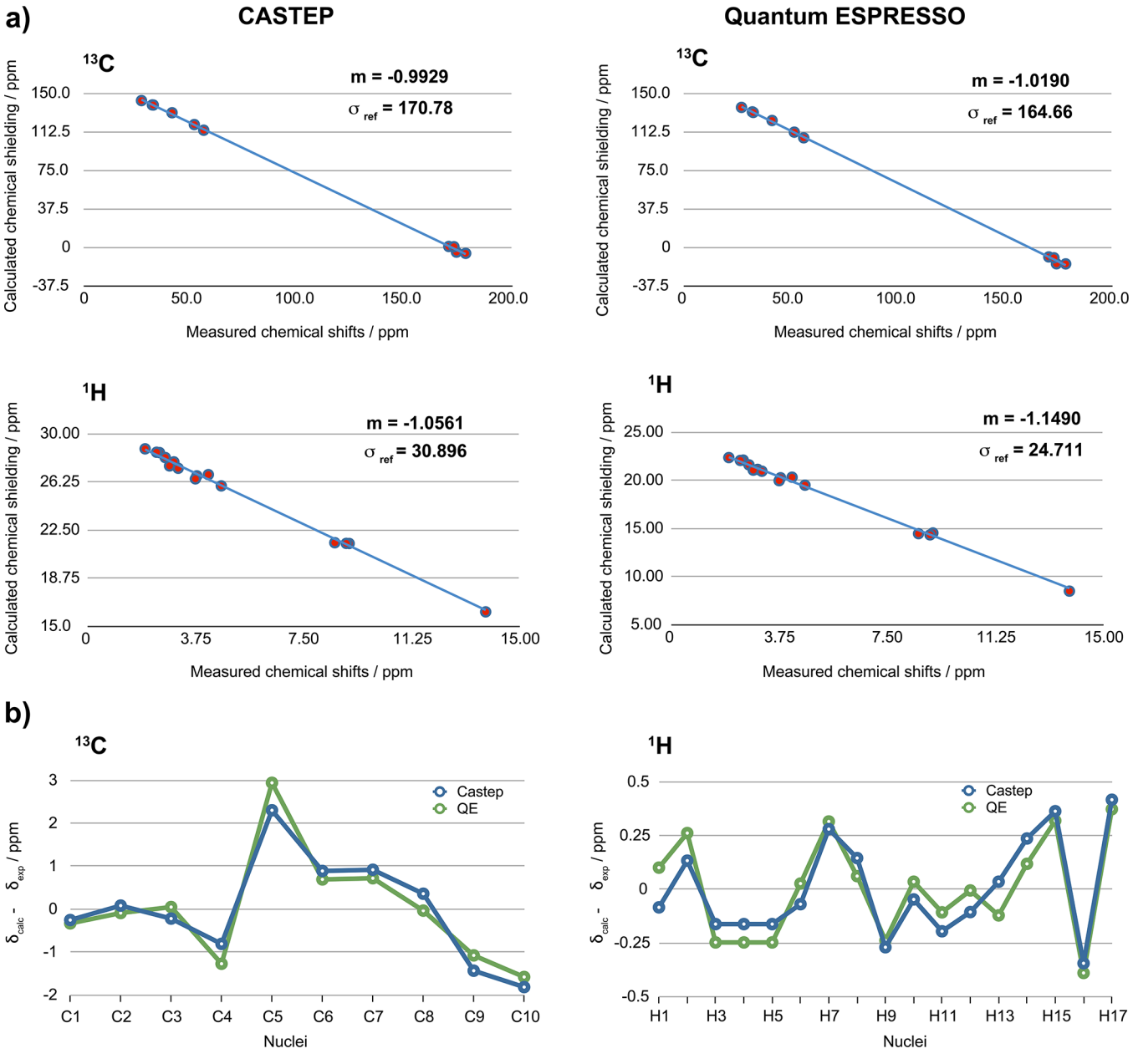

Figure 2. (a) Calculated chemical shieldings versus measured chemical shifts for ^{13}C (top) and ^{1}H (bottom); (b) direct comparison between the results obtained using CASTEP and QE codes ($\delta_{calc} - \delta_{exp}$ plotted as a function of nuclei type).

dx.doi.org/10.1021/jp302128r | J. Phys. Chem. A 2012, 116, 6711−6719

defined within the generalized gradient approximation. All calculations were carried out with version 5.0.1 of the CASTEP code,[4] employing ultrasoft pseudopotentials calculated on the fly; computation of shielding tensors was performed using the GIPAW method of Pickard et al.,[3] which allows chemical shifts to be calculated with an all-electron accuracy within the pseudopotential framework.

The crystal structure of glutathione was obtained from the Cambridge Crystal Database[18] (CSD code GLUTAS02[19]). An initial optimization of the proton positions was conducted with a basis set cutoff of 700 eV and a 4 × 3 × 1 Monkhorst−Pack *k*-point grid (corresponding to a *k*-point spacing of 0.05 Å^{-1}). CASTEP default values for geometry convergence criteria were used.

Calculation of ^{1}H and ^{13}C chemical shieldings was then undertaken on the optimized structure, using the same basis set cutoff and Monkhorst−Pack grid indicated above. Conversion of the calculated isotropic chemical shieldings (σ_{iso}) into the corresponding isotropic chemical shifts (δ_{iso}) was performed according to

$$\delta_{iso} = (\sigma_{iso} - \sigma_{ref})/m$$

where σ_{ref} and m were determined by fitting σ_{iso} to the measured chemical shifts (δ_{exp}) by means of a linear regression (σ_{ref} and m are the intercept and slope of the regression model, respectively).[9]

Quantum ESPRESSO Calculations. The QE calculations considered version 4.0.3[10] of the code and followed a recipe similar to that employed with the CASTEP code. The calculations were performed with the PBE exchange−correlation functional and consisted of a preliminary optimization of the positions of the protons of the GLUTAS02 system (CSD code) followed by calculation of the NMR data within the GIPAW technique. The pseudopotentials of the norm-conserving Troullier−Martins type with GIPAW reconstruction were taken from elsewhere.[20] The cutoff energy for the plane waves and the Monkhorst−Pack *k*-points grid used were 90 Ryd and 4 × 3 × 1, respectively. QE default values for convergence criteria were used.

Calculated chemical shieldings versus measured chemical shifts for ^{13}C and ^{1}H nuclei using CASTEP and QE codes are depicted in Figure 2. Both theoretical methods afforded very good agreement with the experimental data (cf. Results and Discussion).

NMR Experiments. The spectra were acquired on Bruker Avance III 400 and 800 spectrometers operating at a B_0 field of respectively 9.4 and 18.8 T. The ^{1}H and ^{13}C Larmor frequencies were 400.1, 100.6 MHz and 800.3, 201.3 MHz for both magnetic fields, respectively. The ^{14}N experiment was recorded at 18.8 T at the Larmor frequency of 57.8 MHz. All of the NMR experiments were performed at spinning rates in the range of 10−30 kHz. ^{1}H scaling factors were determined by comparing ^{1}H DUMBO[21] and ^{1}H single-pulse (at high spinning rates) spectra. ^{1}H and ^{13}C were referenced with respect to glycine (NH_3^+ at 8.35 ppm and C═O at 176.03 ppm). ^{14}N was referenced using a saturated solution of NH_4Cl (−352.9 ppm corresponding to a primary reference of CH_3NO_2 at 0 ppm).

At 9.4 T, experiments were acquired using a double-resonance 4 mm Bruker MAS probe. The ^{1}H 90 and 180° pulses were set to 3.8 and 7.6 μs, corresponding to a radio frequency (RF) field strength of 66 kHz. The ^{13}C 90 and 180° pulses were set to 3.9 and 7.8 μs, corresponding to an RF field strength of 64 kHz. The CPMAS experiment was acquired using a contact time of

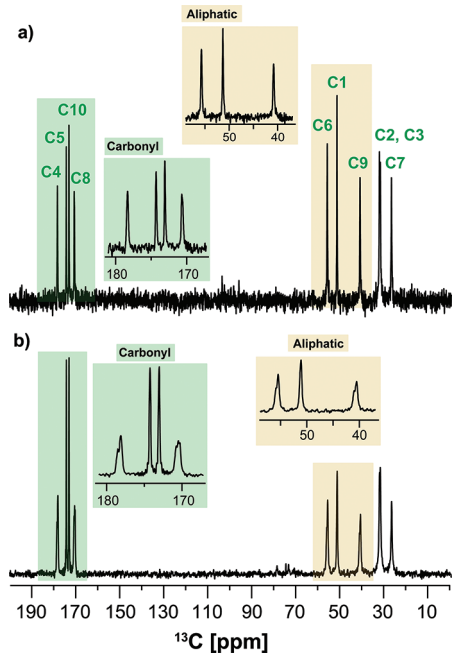

Figure 3. ^{13}C CPMAS NMR spectra of GSH recorded at B_0 = (a) 18.8 and (b) 9.4 T with 15 and 10 kHz MAS, respectively. Two regions (170−180 and 40−60 ppm) of the ^{13}C spectra are highlighted where the effect of ^{14}N in the peak shape is observable.

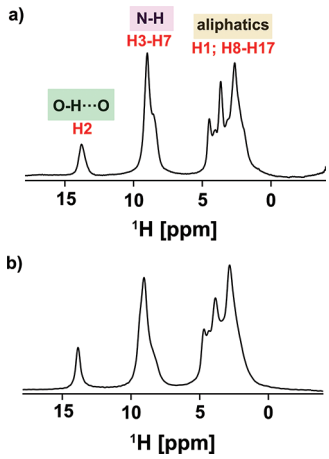

Figure 4. 1D ^{1}H DUMBO$^{x\bar{x}}$ MAS NMR spectra of GSH recorded at (a) B_0 = 18.8 T (800 MHz ^{1}H) and 15 kHz, (b) B_0 = 9.4 T (400 MHz ^{1}H), and 10 kHz MAS.

3.0 ms with ^{1}H and ^{13}C RFs of 90 (50−100% RAMP-CP shape) and 64 kHz, respectively. To record one-dimensional (1D) ^{1}H high-resolution NMR spectra, a windowed DUMBO pulse shape using the *z*-rotation supercycle (wDUMBO$^{x\bar{x}}$)[22] was employed with a pulse length of 30.0 μs, a RF field strength of 100 kHz, and 5.6 μs windows. For the ^{1}H−^{13}C PRESTO-HETCOR experiment, a PRESTO-II[23] magnetization transfer based on the R18$_1^7$ rotor-synchronized symmetry was used, employing an incomplete cycle of sixteen 180° pulses; ^{1}H homonuclear decoupling during t_1 was accomplished using wDUMBO$^{x\bar{x}}$ with the same experimental conditions as those described above. The ^{1}H−^{13}C INEPT-HSQC (*J* coupling) experiment was recorded with a windowed DUMBO$^{x\bar{x}}$ (wDUMBO$^{x\bar{x}}$) decoupling during the indirect dimension (t_1). A standard windowless DUMBO was used during the *J*-coupling evolutions ($\tau = 6\tau_r$; see Figure 5).

dx.doi.org/10.1021/jp302128r | J. Phys. Chem. A 2012, 116, 6711−6719

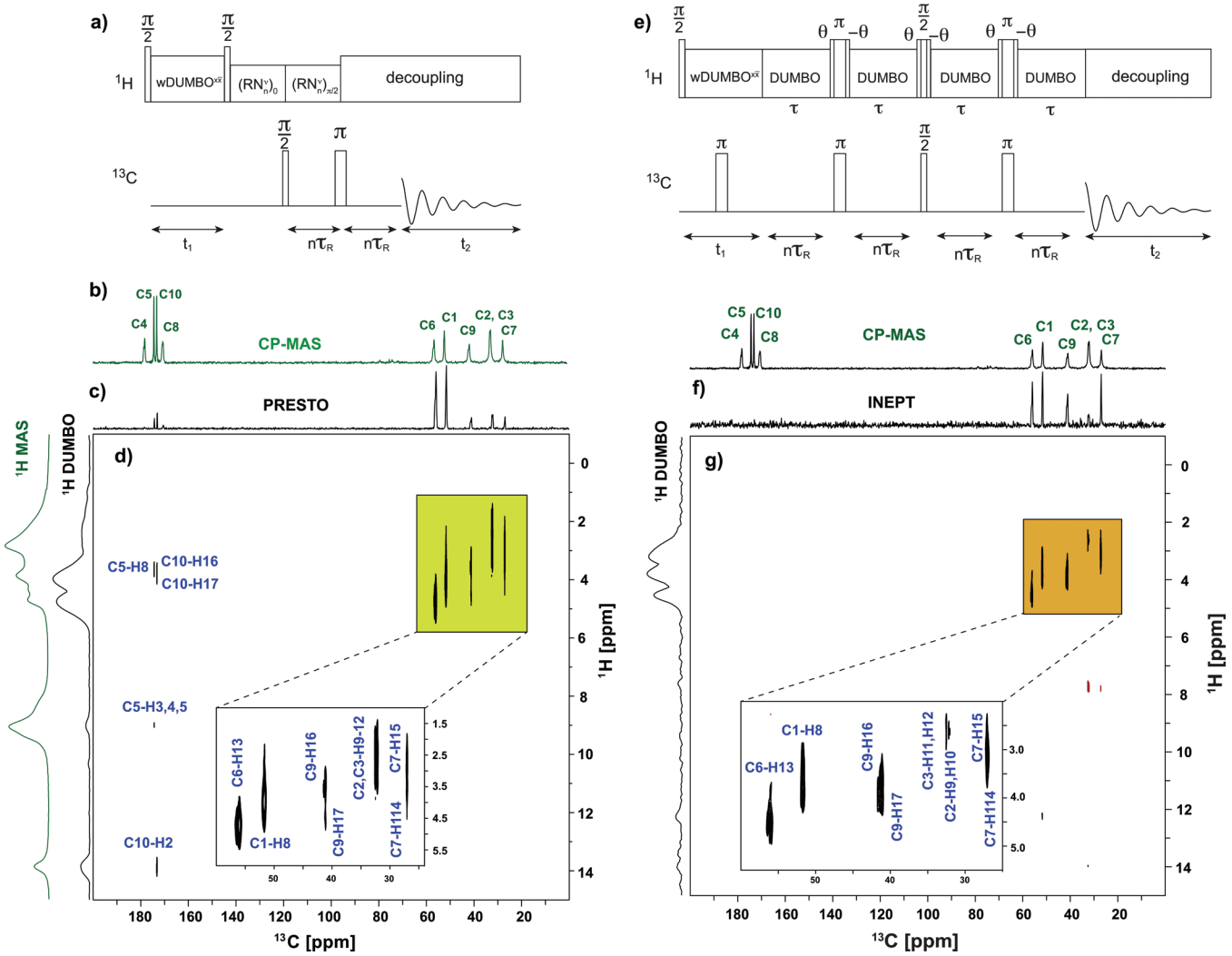

Figure 5. (a) Pulse sequence used for the acquisition of 2D ^{1}H−^{13}C PRESTO-HETCOR NMR spectrum of GSH recorded at B_0 = 9.4 T and a MAS rate of 10 kHz; (b) ^{13}C CPMAS recorded under the same conditions; (c) ^{13}C PRESTO projection along the F2 dimension; and (d) the 2D ^{1}H−^{13}C PRESTO-HETCOR spectrum. The ^{1}H 1D DUMBO spectrum is also shown along the F1 dimension for comparison. The acquisition parameters are the following: 64 t_1 points with 80 scans each were acquired along the F1 dimension; total mixing time of 178 μs for the two RN_n^{ν} blocks; and recycle delay (RD) = 4 s. (e) Pulse sequence used for the acquisition of the 2D ^{1}H−^{13}C INEPT-HSQC HETCOR spectrum of GSH recorded at B_0 = 9.4 T and a MAS rate of 10 kHz, employing τ = 1.2 ms (=6τ_r) corresponding to 40 DUMBO decoupling blocks; f) ^{13}C INEPT-HSQC projection along the F2 dimension; and (g) 2D ^{1}H−^{13}C INEPT-HSQC spectrum with the following acquisition parameters: 64 t_1 points with 192 scans each were acquired along the F1 dimension; RD = 4 s. Both experiments used a dwell time in F1 of 284.8 μs, equivalent to four wDUMBO$^{x\bar{x}}$ supercycles.

During the acquisition of the ^{13}C signal, a SPINAL-64[24] decoupling with a RF field strength of 100 kHz was employed.

At 18.8 T, the NMR experiments were acquired on triple-resonance 2.5 mm and double-resonance 3.2 mm Bruker MAS probes. The ^{1}H 90 and 180° pulses were set to 2.5 and 5.0 μs, corresponding to a RF field strength of 100 kHz. The 2D ^{1}H−^{1}H DQ−SQ spectrum was acquired using the $R12_2^5$ symmetry (RF = 90 kHz) for DQ excitation/reconversion and wDUMBO$^{x\bar{x}}$ decoupling during t_1 and t_2 evolutions. A shape length of 16.0 μs, decoupling power of 150 kHz, and windows of 5.6 μs were used for wDUMBO$^{x\bar{x}}$. The ^{13}C CPMAS experiment used a RF field strength of 77 kHz for ^{13}C while the ^{1}H channel was ramped from 50 to 100% in power level (RF = 71 kHz as the maximum). The 1D ^{1}H CRAMPS spectrum was acquired using the wDUMBO$^{x\bar{x}}$ shape pulse length of 37.5 μs and a RF field strength of 75 kHz; windows were set to 5.6 μs. The ^{1}H−^{14}N *D*-HMQC spectrum was recorded employing a complete $SR4_1^2$ symmetry[25] (24 π pulses with RF(^{1}H) = 40 kHz) for the transfer of coherence order from ^{1}H to ^{14}N spins. The two ^{14}N pulses were set to 20.0 μs length using RF ≈ 67 kHz (calibrated from NH_4Cl), corresponding to the maximum ^{14}N signal intensity. A rotor-synchronized t_1 evolution was employed between two ^{14}N pulses.

RESULTS AND DISCUSSION

^{13}C Resonance Assignment. The 1D ^{13}C CPMAS spectra of GSH (Figure 3) exhibit six (C1−C3, C6, C7, and C9) well-resolved resonances between 20 and 70 ppm for the six aliphatic carbons and four resonances (C4, C5, C8, and C10) for the carbonyl groups centered at 175 ppm, in agreement with the known crystal structure,[19] which calls for a single molecule in the asymmetric unit (Z' = 1). Therefore, 10 carbons and 17 proton resonances are expected in the ^{13}C and ^{1}H (Figure 4) NMR spectra, respectively.

The comparison of the ^{13}C CPMAS spectra acquired at two distinct magnetic fields [B_0 = 18.8 (Figure 3a) and 9.4 T

dx.doi.org/10.1021/jp302128r | J. Phys. Chem. A 2012, 116, 6711−6719

Table 1. Experimental ^{13}C, ^{1}H, and ^{15}N Chemical Shifts (δ_{iso}) of Glutathione and Corresponding Values Determined Using Quantum ESPRESSO (QE) and CASTEP Calculation Tools

atom label	exp. δ_{iso} (ppm)	calc. δ_{iso} (ppm) QE*	rmsd	calc. δ_{iso} (ppm) CASTEP*	rmsd
C1	51.70	51.37 (−0.33)	0.11	51.44 (−0.26)	0.07
C2	32.10	32.01 (−0.09)	0.01	32.18 (0.08)	0.01
C3	32.50	32.55 (0.05)	0.00	32.28 (−0.22)	0.05
C4	178.60	177.33 (−1.27)	1.62	177.79 (−0.81)	0.66
C5	174.30	177.24 (2.94)	8.65	176.60 (2.30)	5.29
C6	56.10	56.79 (0.69)	0.48	56.99 (0.89)	0.79
C7	27.00	27.72 (0.72)	0.52	27.92 (0.92)	0.84
C8	170.70	170.66 (−0.04)	0.00	171.06 (0.36)	0.13
C9	41.30	40.22 (−1.08)	1.16	39.86 (−1.44)	2.06
C10	173.10	171.52 (−1.58)	2.50	171.28 (−1.82)	3.30
H1	3.00	3.10 (0.10)	0.01	2.92 (0.08)	0.01
H2	13.85	14.11 (0.26)	0.07	13.98 (0.13)	0.02
H3, H4, H5	9.10	8.85 (−0.25)	0.06	8.93 (0.17)	0.03
H6	9.00	9.03 (0.03)	0.00	8.93 (0.07)	0.00
H7	8.60	8.91 (0.31)	0.10	8.88 (0.28)	0.08
H8	3.80	3.86 (0.06)	0.00	3.95 (0.15)	0.02
H9	2.50	2.26 (−0.24)	0.06	2.23 (0.27)	0.07
H10	2.00	2.04 (0.04)	0.00	1.95 (0.05)	0.00
H11	2.40	2.29 (−0.11)	0.01	2.21 (0.19)	0.04
H12	2.70	2.70 (0.00)	0.00	2.60 (0.10)	0.01
H13	4.65	4.53 (−0.12)	0.01	4.69 (0.04)	0.00
H14	3.15	3.27 (0.12)	0.01	3.39 (0.24)	0.06
H15	2.85	3.17 (0.32)	0.10	3.21 (0.36)	0.13
H16	3.75	3.81 (−0.39)	0.15	3.85 (−0.35)	0.12
H17	4.20	4.12 (0.37)	0.14	4.17 (0.42)	0.17
N1	−347.75	−348.06 (−0.31)	0.09	−348.06 (−0.32)	0.10
N2	−265.52	−267.42 (−1.91)	3.64	−267.42 (−1.98)	3.93
N3	−276.92	−274.71 (2.22)	4.91	−274.62 (2.30)	5.30

*($\delta_{calc.}$ - $\delta_{exp.}$) indicated between brackets. Positive values refer to overestimated $\delta_{calc.}$ and negative values refer to underestimated $\delta_{calc.}$

(Figure 3b)] allows unambiguous assignment of at least four C−N resonances (C4, C6, C8, and C9) as these carbon environments typically appear as asymmetric doublets at lower magnetic fields (Figure 3b). The observation of doublets in the ^{13}C spectrum arises from the residual $^{13}C-^{14}N$ dipolar couplings caused by the quadrupole interaction of the neighboring ^{14}N integer spins. This line splitting is a well-described phenomenon.[26] At higher B_0 fields, this effect vanishes because the strong quadrupolar coupling interaction of ^{14}N is inversely proportional to the B_0 field. Thus, ^{13}C resonances corresponding to carbons directly bonded to nitrogens resonate at 178.6 (C4), 170.7 (C8), 56.1 (C6), 41.3 (C9), and 51.7 (C1) ppm. The latter resonance (C1) exhibits a negligible splitting, indicating that the ^{13}C is most likely next to the NH_3^+ nitrogen group, which usually has a smaller quadrupolar coupling constant (C_Q) than amide functional groups HN−C═O (NH_3^+ groups often have $C_Q \approx 1$ MHz, while amides typically present C_Q's of 3−5 MHz[27]).

The complete assignment of carbon resonances, particularly those given by the carboxylic groups (C5 and C10), is assisted by 2D high-resolution $^{1}H-^{13}C$ HETCOR NMR spectra using $R18_1^7$ (PRESTO) (Figure 5d) and INEPT (Figure 5g) magnetization transfers.

In previous works, *J*-coupling based NMR techniques (HMQC and INEPT) were used to probe one-bond connectivity between hydrogen and carbon nuclei. Using such techniques, multiple 2D experiments, with distinct *J*-coupling evolution periods, are frequently required to tune the selectivity between CH, CH_2, and CH_3 groups.[28] In a recent contribution,[9] we have shown that the use of a PRESTO transfer affords equivalent selectivity, allowing only selection of the directly bonded carbons and hydrogens using a single experiment; quaternary carbons were completely filtered out from the ^{13}C spectra. Moreover, PRESTO is dipolar-based and therefore more sensitive than *J*-coupling based experiments; for instance, the acquisition time to record a $^{1}H-^{13}C$ PRESTO-HETCOR spectrum (Figure 5d) was half of the time needed to record a $^{1}H-^{13}C$ INEPT-HSQC spectrum (Figure. 5g).

In Figure 5c, the F2 projection of the $^{1}H-^{13}C$ PRESTO HETCOR spectrum shows that quaternary carbons (C4, C5, C8, and C10) are nearly filtered out when compared to ^{13}C CPMAS (Figure 5b). Although the $^{1}H-^{13}C$ INEPT-HSQC, this time, performed slightly better in removing the carbonyls' resonances, C2 and C3 CH_2 resonances are barely observable, as compared to PRESTO. Because the C2 and C3 chemical shift values (δ_C = 32.10 and 32.50 ppm, respectively) are almost the same due to the similar chemical surroundings, their unambiguous assignment is only possible with the help of the GIPAW chemical shifts (Table 1). For the sake of comparison, the $^{1}H-^{13}C$ PRESTO-HETCOR (Figure 5d) and INEPT-HSQC NMR (Figure 5g) spectra are shown side-by-side, but only the former spectrum will be used in the following discussion.

Although the H2 proton, involved in the strong OH···O hydrogen bond, is well-resolved from the simple 1D ^{1}H DUMBO spectrum (Figure 4), the aliphatic ^{1}H region shows insufficient resolution. To overcome this inconvenience, we

dx.doi.org/10.1021/jp302128r | J. Phys. Chem. A 2012, 116, 6711−6719

profit from the discrimination capability (i.e., large ^{13}C chemical shift dispersion) inherent to the 2D $^{1}H-^{13}C$ HETCOR spectra for the assignment task. The strategy for the assignment of the ^{1}H resonances is now discussed in detail.

^{1}H Resonance Assignment. The ^{1}H spectra consist of three distinct domains (Figure 4), the aliphatic protons appearing at $\delta_H \approx 0-5$ ppm, the N−H protons around 9 ppm, and the ^{1}H resonance at $\delta_H \approx 14$ ppm, attributed to the O−H···O hydrogen bond. The assignment of the 17 ^{1}H resonances is achieved by combining information derived from 2D $^{1}H-^{1}H$ DQ-CRAMPS, $^{1}H-^{13}C$ PRESTO-HETCOR, and $^{1}H-^{14}N$ *D*-HMQC spectra. GIPAW ^{1}H chemical shift calculations are used to validate the assignments and help solve ambiguities (Table 1).

From the *D*-HMQC $^{1}H-^{14}N$ displayed in Figure 6, it is possible to distinguish two separate N−H environments, a broad

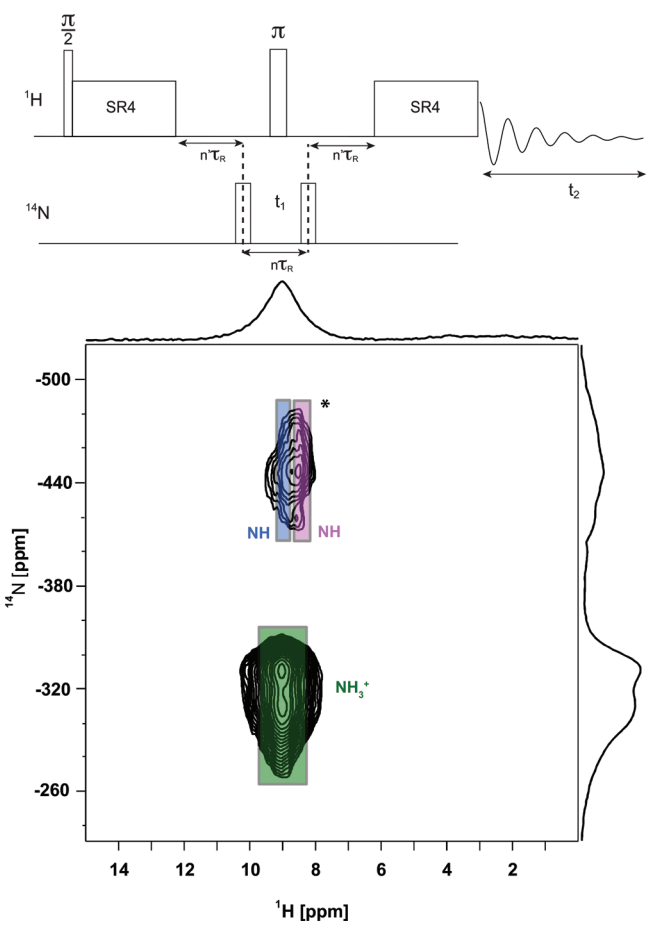

Figure 6. 2D $^{1}H-^{14}N$ dipolar-HMQC spectrum of GSH recorded at $B_0 = 18.8$ T and using a MAS rate of 20 kHz. The corresponding pulse sequence is displayed at the top. 64 t_1 points with 16 scans each were acquired along the F1 dimension; a pulse length of 300 μs was used for excitation and reconversion blocks; RD = 5 s. (*) N−H resonances are folded (see text).

^{14}N resonance centered at −325 ppm ascribed to the NH_3^+ group (with protons H3−5 at ∼9.10 ppm) and another ^{14}N peak centered at −445 ppm assigned to the two overlapping amide N−H resonances (H6 and H7 with $\delta_H = 9.00$ and 8.60 ppm, respectively). The later $^{14}N-^{1}H$ cross-peak, shows an asymmetry along the ^{1}H dimension, suggesting the presence of the two distinct H6 and H7 proton environments (see highlighted boxes in Figure 6). It is worth mentioning that the N−H amide resonances are aliased and thus appear displaced from the expected calculated ^{14}N chemical shift position (see Table S2, Supporting Information).

To support our assignment of $^{1}H-^{14}N$ *D*-HMQC, we have also recorded 1D ^{15}N CP-MAS (see Supporting Information Figure S1). It is possible to identify $\delta_{iso}(N-H) = -265.5$ and −276.9 ppm and $\delta_{iso}(NH_3^+) = -347.8$ ppm. The isotropic contribution of the second-order quadupolar interaction sums with the isotropic chemical shift, explaining the peak shifting between $\delta_{iso}(^{14}N)$ and $\delta_{iso}(^{15}N)$. Quadrupolar coupling constants (C_Q) are on the order of −3.4, −3.3, and 1.4 for the two N−H and NH_3 groups, calculated as reported by others[29] (see Supporting Information Tables S1 and S2). This approach is useful to explain the position of the ^{14}N peaks in the indirect dimension.

The 2D $^{1}H-^{13}C$ PRESTO-HETCOR spectrum (Figure 5d) contains all of the cross-peaks corresponding to the CH and CH_2 groups, showing additional small cross-peaks for some larger C···H distances involving the carbonyls. This 2D spectrum confirms some of the assignments done previously for the ^{13}C chemical shifts and allows for a first estimation of the ^{1}H isotropic chemical shifts. As an example, the C═O at 173.10 ppm is assigned to C10 because this carbon is expected to present a correlation with H2 protons at 13.85 ppm, as highlighted in Figure 5d, due to their proximity (Figure 1). Likewise, the C═O (C5) at 174.30 ppm shows correlations both with the NH_3^+ protons (H3−5) at 9.10 ppm and a CH (H8) proton as these sites are the closest to C5. In addition, the following ^{1}H resonance assignments are obtained from the spectral analysis of the $^{1}H-^{13}C$ HETCOR NMR spectra: H8 at 3.80 ppm, H13 at 4.65 ppm, H9−H12 between 1.90 and 3.00 ppm, H14/H15 at 2.70−3.30 ppm, and H16/H17 at 3.50−4.50 ppm. It is worth mentioning that the PRESTO transfer permits one to easily distinguish CH from CH_2 carbons as the former gives resonances more intense than the latter (see the top projection in Figure 5c). This is due to the stronger dipolar dephasing of the CH_2 relative to CH groups during the PRESTO recoupling time (also observed by other authors[5,28]) a feature that may be used for spectral editing, further aiding the ^{1}H resonances assignment. The remaining assignments followed the same strategy, and full details are given in Table 1.

The potential of multiple-quantum MAS NMR spectroscopy, particularly DQ MAS, for the characterization of solids is well-established.[9,30] The use of 1D ^{1}H MAS and 2D $^{1}H-^{1}H$ DQ recoupling experiments, employing fast MAS alone (∼30 kHz)[30c] and combined with CRAMPS decoupling,[31] affords enough resolution to study hydrogen bonds and $\pi\cdots\pi$ stacking effects in crystalline systems. ^{1}H DQ spectroscopy has been applied extensively to investigate hydrogen-containing solids, to obtain proton−proton proximities within 3.5 Å for a typical organic solid.[32] Figure 7 shows the 2D $^{1}H-^{1}H$ DQ-CRAMPS spectrum of GSH, used in combination with the $^{1}H-^{13}C$ PRESTO-HETCOR and $^{1}H-^{14}N$ *D*-HMQC to fully assign all ^{1}H isotropic chemical shifts. The geminal protons from each CH_2 group are expected to exhibit strong cross-peaks, enabling their identification (2.00/2.50 ppm for H10/H9, 2.40/2.70 ppm for H11/H12, 2.85/3.15 ppm for H15/H14, and 3.75/4.2 ppm for H16/H17; see Figure 7 where some of these correlations are marked). The three NH_3^+ protons appear as a single and strong diagonal cross-peak at $\delta_{SQ} = 9.1$, $\delta_{DQ} = 18.2$ ppm. The two remaining NH protons resonate at 9.0 (H7) and 8.6 ppm (H6). The assignment of H1 to the SH

dx.doi.org/10.1021/jp302128r | J. Phys. Chem. A 2012, 116, 6711−6719

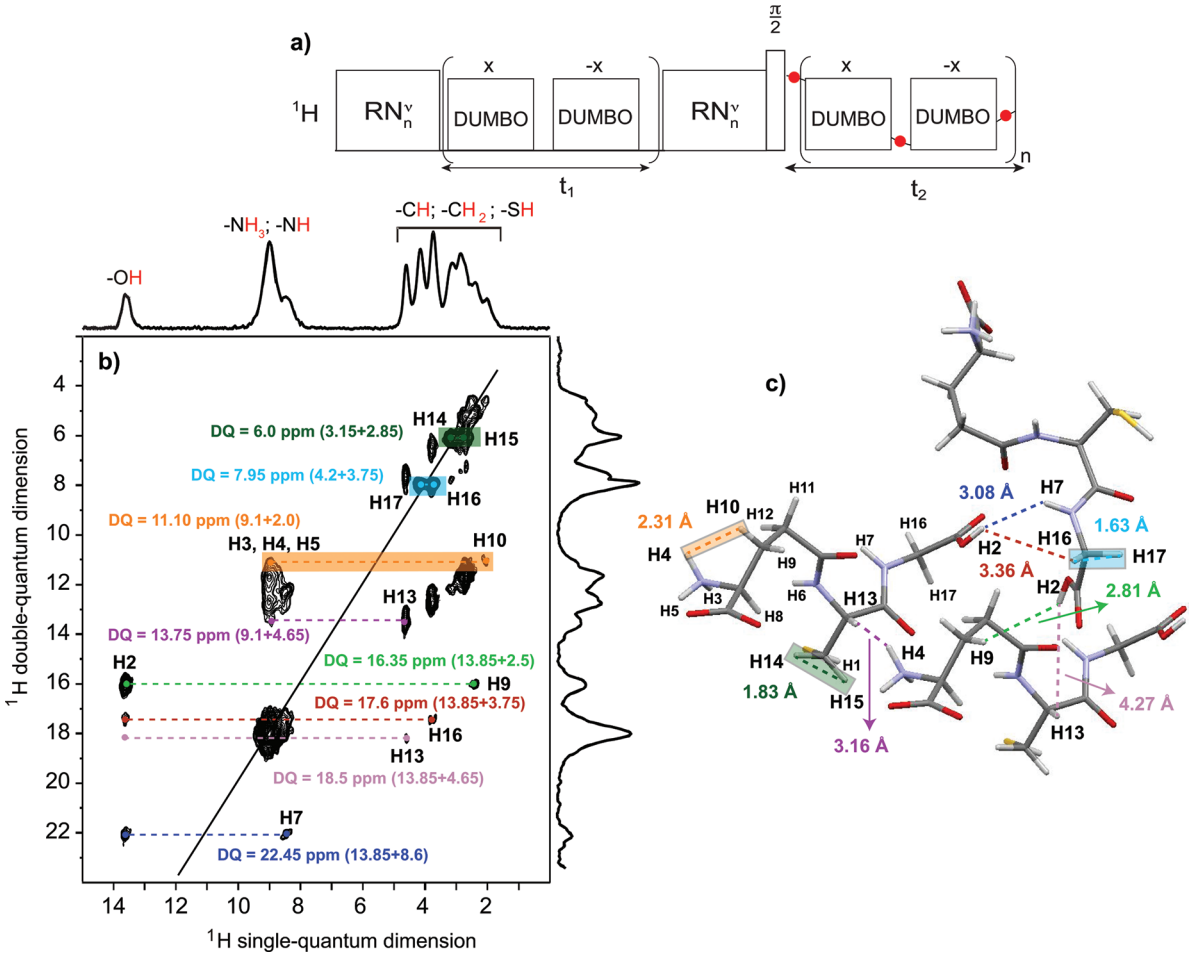

Figure 7. (a) Pulse sequence used for the acquisition of (b) the 2D ^{1}H−^{1}H DQ-SQ CRAMPS spectrum of GSH recorded at B_0 = 18.8 T and a MAS rate of 30 kHz. Intramolecular correlations are highlighted inside of colored boxes both in the spectrum and the crystal structure scheme depicted in (c). All of the other selected nuclear distances highlighted in the figure correspond to intermolecular contacts. 302 t_1 points with 32 scans each were acquired along the F1 dimension; total excitation and reconversion times of 66.7 μs were used; RD = 3 s; dwell time in F1 was 43.2 μs, equivalent to one wDUMBO$^{\bar{x}\bar{x}}$ supercycle.

resonances at 3.0 ppm was corroborated with the calculated ^{1}H chemical shifts (Table 1). In order to unambiguously assign each ^{1}H resonance, the nearest neighbors are examined, starting with the analysis of the well-separated OH peak (H2 at 13.85 ppm). From the 2D spectrum, the H2 proton is involved in various off-diagonal DQ−SQ cross-peaks, showing its spatial proximity to other protons with distinct chemical environments. According to the GSH crystal structure, the closest neighbors of H2 are H11 (2.30 Å), H9 (2.81 Å), H7 (3.08 Å), and H16 (3.36 and 3.43 Å) (Table 2). The H2 proton is indeed involved in different off-diagonal DQ−SQ cross-peaks, indicating its proximity to other protons with distinct chemical environments. These cross-peaks appear at δ_{DQ} = 16.25 ppm (H2···H11), δ_{DQ} = 16.35 ppm (H2···H9), δ_{DQ} = 22.45 ppm (H2···H7), and δ_{DQ} = 17.60 ppm (H2···H16) for the intermolecular correlations (Figure 7; only some of these correlations are highlighted for clarity). Hence, H7 shows at 8.6 ppm, H16 shows at 3.75 ppm, and H9 and H11 show at 2.5 or 2.4 ppm, respectively. Consideration of the H···H distances from the crystal structure and the presence/absence of DQ−SQ cross-peaks allows the differentiation between H16 and H17 as the latter does not correlate with H2. Using the same rationale for all of the remaining protons of GSH, it is possible to assign most ^{1}H chemical shifts. Exceptions are H9−12 protons that were only reliably assigned comparing the experimental and theoretical chemical shifts (see Tables 1 and 2).

CONCLUSION

The full assignment of the NMR spectra of model compound GSH was accomplished using a combination of ^{1}H, ^{13}C, and ^{14}N solid-state NMR techniques and first-principles calculations of ^{1}H and ^{13}C chemical shifts with the GIPAW modules of the CASTEP and QE codes. This approach may be extended to other organic compounds. The two methods used for theoretical determination of ^{1}H and ^{13}C chemical shifts yield results in good agreement with the experimental data. The discrepancies between the calculated and experimental ^{1}H and ^{13}C chemical shifts were smaller than 0.36 and 2.30 ppm, respectively, using CASTEP and smaller than 0.32 and 2.94 ppm, respectively, using QE.

The use of high-resolution multiple-pulse ^{1}H-based NMR experiments at high magnetic fields combined with first-principles calculations of NMR parameters allows the full assignment of NMR resonance of powdered samples. GSH is a tripeptide having many identical functional groups, that is, various CH_2, CH, and NH groups containing several geminal and vicinal protons, whose resonances often overlap, and thus, it constitutes an interesting challenge. A number of

dx.doi.org/10.1021/jp302128r | J. Phys. Chem. A 2012, 116, 6711−6719

Table 2. List of ^{1}H δ_{iso} and δ_{DQ} Assembled from the Experimental δ_{iso} and δ_{DQ} Values[a]

proton type (functional group)	δ_{iso} (ppm)	δ_{DQ} (in ppm) and corresponding protons with their distances (up to 3.5 Å)
H1 (SH)	3.00	5.85 (H1···H15: 2.29 Å)
		12.10 (H1···H3/H4/H5: 2.69 Å)
		6.15 (H1···H14: 3.13 Å)
		7.65 (H1···H13: 3.17 Å)
		5.85 (H1···H15: 2.29 Å)
		6.80 (H1···H8: 3.46 Å)
H2 (OH)	13.85	16.25 (H2···H11: 2.30 Å)
		16.35 (H2···H9: 2.81 Å)
		22.45 (H2···H7: 3.08 Å)
		17.60 (H2···H16: 3.36 Å)
		18.50 (H2···H13: 4.27 Å)
H3,H4, H5 (NH_3^+)	9.10	18.20 (H3/H4/H5···H3/H4/H5: 1.31−1.49Å)
		12.90 (H3/H4/H5···H8: 2.04 Å)
		11.80 (H3/H4/H5···H12: 2.58 Å)
		12.10 (H3/H4/H5···H1: 2.69 Å)
		18.10 (H3/H4/H5···H6: 3.00 Å)
		11.10 (H3/H4/H5···H10: 2.31 Å)
		11.95 (H3/H4/H5···H15: 2.32 Å)
		13.75 (H3/H4/H5···H13: 3.16 Å)
		11.60 (H3/H4/H5···H9: 3.47 Å)
H6 (NH)	9.00	11.70 (H6···H12: 2.29 Å)
		12.15 (H6···H14: 2.31 Å)
		13.65 (H6···H13: 2.51 Å)
		17.60 (H6···H7: 2.63 Å)
		12.80 (H6···H8: 2.78 Å)
		18.10 (H6···H3/H4/H5: 3.00 Å)
		11.50 (H6···H9: 3.18 Å)
		11.40 (H6···H11: 3.39 Å)
		11.85 (H6···H15: 3.48 Å)
H7 (NH)	8.60	12.35 (H7···H16: 2.21 Å)
		17.60 (H7···H6: 2.63 Å)
		12.80 (H7···H17: 2.83 Å)
		22.45 (H7···H2: 3.08 Å)
		13.25 (H7···H13: 3.11 Å)
H8 (CH)	3.80	12.90 (H8···H3/H4/H5: 2.04 Å)
		6.30 (H8···H9: 2.55 Å)
		12.80 (H8···H6: 2.78 Å)
		~~6.95 (H8···H14: 2.81 Å)~~
		5.80 (H8···H10: 2.85 Å)
		6.20 (H8···H12: 2.96 Å)
		6.65 (H8···H15: 3.38 Å)
		8.45 (H8···H13: 3.41 Å)
		6.80 (H8···H1: 3.46 Å)
H9 (CH_2)	2.50	*4.50 (H9···H10: 1.52 Å)*
		4.90 (H9···H11: 2.38 Å)
		6.30 (H9···H8: 2.55 Å)
		5.20 (H9···H12: 2.71 Å)
		16.35 (H9···H2: 2.81 Å)
		6.70 (H9···H17: 2.87 Å)
		11.50 (H9···H6: 3.18 Å)
		11.6 (H9···H3/H4/H5: 3.47 Å)
H10 (CH_2)	2.00	*4.50 (H10···H9: 1.52 Å)*
		6.20 (H10···H17: 2.18 Å)
		11.10 (H10···H3/H4/H5: 2.31 Å)
		4.40 (H10···H11: 2.34 Å)
		4.70 (H10···H12: 2.43 Å)
		5.80 (H10···H8: 2.85 Å)
		~~5.75 (H10···H16: 3.38 Å)~~
H11 (CH_2)	2.40	5.10 (H11···H12: 1.72 Å)
		16.25 (H11···H2: 2.30 Å)
		4.40 (H11···H10: 2.34 Å)
		4.90 (H11···H9: 2.38 Å)
		6.15 (H11···H16: 3.02 Å)
		11.40 (H11···H6: 3.39 Å)
H12 (CH_2)	2.70	5.10 (H12···H11: 1.72 Å)
		11.70 (H12···H6: 2.29 Å)
		4.70 (H12···H10: 2.43 Å)
		11.80 (H12···H3/H4/H5: 2.58 Å)
		5.20 (H12···H9: 2.92 Å)
		6.50 (H12···H8: 2.96 Å)
		7.35 (H12···H13: 4.23 Å)
H13 (CH)	4.65	7.80 (H13···H14: 2.24 Å)
		7.50 (H13···H15: 2.28 Å)
		13.65 (H13···H6: 2.51 Å)
		13.25 (H13···H7: 3.11 Å)
		13.75 (H13···H3/H4/H5: 3.16 Å)
		7.65 (H13···H1: 3.17 Å)
		8.40 (H13···H16: 3.40 Å)
		8.45 (H13···H8: 3.41 Å)
		18.50 (H13···H2: 4.27 Å)
H14 (CH_2)	3.15	6.00 (H14···H15: 1.83 Å)
		7.80 (H14···H13: 2.24 Å)
		12.15 (H14···H6: 2.31 Å)
		~~6.95 (H14···H8: 2.81 Å)~~
		6.15 (H14···H1: 3.13 Å)
H15 (CH_2)	2.85	6.00 (H15···H14: 1.83 Å)
		7.50 (H15···H13: 2.28 Å)
		5.85 (H15···H1: 2.29 Å)
		11.95 (H15···H3/H4/H5: 2.32 Å)
		6.65 (H15···H8: 3.38 Å)
		11.85 (H15···H6: 3.48 Å)
H16 (CH_2)	3.75	7.95 (H16···H17: 1.63 Å)
		12.35 (H16···H7: 2.21 Å)
		6.15 (H16···H11: 3.02 Å)
		17.6 (H16···H2: 3.36 Å)
		~~5.75 (H16···H10: 3.38 Å)~~
		8.40 (H16···H13: 3.40 Å)
H17 (CH_2)	4.20	7.95 (H17···H16: 1.63 Å)
		6.20 (H17···H10: 2.18 Å)
		12.80 (H17···H7: 2.83 Å)
		6.70 (H17···H9: 2.87 Å)

[a]Italicized text indicates the proton resonances not unambiguously assigned from the experimental NMR data (overlapped in Figure 7). These correlations were inferred from the combined analysis of experimental chemical shifts and X-ray structure. The shortest H···H distances are shown inside of the parentheses. Strikethrough text indicates non-observed correlations.

conclusions were derived from this study. For example, we pointed out that recording 1D NMR spectra at different B_0 fields might assist in the assignment of C−N carbons. ^{1}H−^{14}N HETCOR experiments were also useful to assign the distinct protons attached to the nitrogen atoms. In addition, combining ^{1}H−^{13}C PRESTO-HETCOR and ^{1}H−^{13}C INEPT-HSQC NMR spectra is advantageous as they present distinct selectivity toward CH and CH_2 carbon resonances, thus

dx.doi.org/10.1021/jp302128r | J. Phys. Chem. A 2012, 116, 6711−6719

contributing as an extra discrimination tool for the resonance assignment exercise.

■ ASSOCIATED CONTENT

Supporting Information

1D ^{15}N spectrum of GSH as well as tables listing the full calculated CSA components for all nuclei and the quadrupolar interaction properties for ^{14}N. This material is available free of charge via the Internet at http://pubs.acs.org.

■ AUTHOR INFORMATION

Corresponding Author

*Fax: +351 234 401 470. E-mail: lmafra@ua.pt.

Notes

The authors declare no competing financial interest.

■ ACKNOWLEDGMENTS

We thank FCT, QREN, COMPETE, and EU for financial support and postdoc grants for M.S. (SFRH/BPD/65978/2009), R.S. (SFRH/BPD/44355/2008) and S.M.S. (SFRH/BPD/64752/2009). The Portuguese NMR Network (RNRMN) is acknowledged for granting access to the 18.8 T NMR Bruker spectrometer at ITQB. FCT is also acknowledged for other funding, R&D Project PTDC/QUI-QUI/100998/2008, Programme Ciência 2007, and PEst-C/CTM/LA0011/2011. L.M. also greatly acknowledges the Campus de Excelencia Internacional Ad Futurum de la Universidad de Oviedo (FUTTALENT Program).

■ REFERENCES

(1) Harris, R. K. *Solid State Sci.* **2004**, *6*, 1025−1037.
(2) (a) Elena, B.; Pintacuda, G.; Mifsud, N.; Emsley, L. *J. Am. Chem. Soc.* **2006**, *128*, 9555−9560. (b) Harris, R. K. *Analyst* **2006**, *131*, 351−373. (c) Offerdahl, T. J.; Salsbury, J. S.; Dong, Z.; Grant, D. J. W.; Schroeder, S. A.; Prakash, I.; Gorman, E. M.; Barich, D. H.; Munson, E. J. *J. Pharm. Sci.* **2005**, *94*, 2591−2605. (d) Portieri, A.; Harris, R. K.; Fletton, R. A.; Lancaster, R. W.; Threlfall, T. L. *Magn. Reson. Chem.* **2004**, *42*, 313−320. (e) Tishmack, P. A.; Bugay, D. E.; Byrn, S. R. *J. Pharm. Sci.* **2003**, *92*, 441−474.
(3) (a) Pickard, C. J.; Mauri, F. *Phys. Rev. B* **2001**, *63*, 245101. (b) Yates, J. R.; Pickard, C. J.; Mauri, F. *Phys. Rev. B* **2007**, *76*, 024401.
(4) Clark, S. J.; Segall, M. D.; Pickard, C. J.; Hasnip, P. J.; Probert, M. I. J.; Refson, K.; Payne, M. C. *Z. Krystallogr.* **2005**, *220* (5−6-2005), 567−570.
(5) Webber, A. L.; Elena, B.; Griffin, J. M.; Yates, J. R.; Pham, T. N.; Mauri, F.; Pickard, C. J.; Gil, A. M.; Stein, R.; Lesage, A.; et al. *Phys. Chem. Chem. Phys.* **2010**, *12*, 6970−6983.
(6) Mifsud, N.; Elena, B.; Pickard, C. J.; Lesage, A.; Emsley, L. *Phys. Chem. Chem. Phys.* **2006**, *8*, 3418−3422.
(7) Uldry, A.-C.; Griffin, J. M.; Yates, J. R.; Perez-Torralba, M.; Santa Maria, M. D.; Webber, A. L.; Beaumont, M. L. L.; Samoson, A.; Claramunt, R. M.; Pickard, C. J.; et al. *J. Am. Chem. Soc.* **2008**, *130*, 945−954.
(8) Bradley, J. P.; Velaga, S. P.; Antzutkin, O. N.; Brown, S. P. *Cryst. Growth Des.* **2011**, *11*, 3463−3471.
(9) Mafra, L.; Santos, S. M.; Siegel, R.; Alves, I.; Almeida Paz, F. A.; Dudenko, D.; Spiess, H. W. *J. Am. Chem. Soc.* **2012**, *134*, 71−74.
(10) Giannozzi, P.; Baroni, S.; Bonini, N.; Calandra, M.; Car, R.; Cavazzoni, C.; Ceresoli, D.; Chiarotti, G. L.; Cococcioni, M.; Dabo, I.; et al. *J. Phys.: Condens. Matter* **2009**, *21*, 395502.
(11) Ukmar, T.; Kaucic, V.; Mali, G. *Acta Chim. Slov.* **2011**, *58*, 425−433.
(12) Thonhauser, T.; Ceresoli, D.; Marzari, N. *Int. J. Quantum Chem.* **2009**, *109*, 3336−3342.
(13) Ceresoli, D.; Marzari, N.; Lopez, M. G.; Thonhauser, T. *Phys. Rev. B* **2010**, *81*, 184424.
(14) Charpentier, T. *Solid State Nucl. Magn. Reson.* **2011**, *40*, 1−20.
(15) (a) Aoyama, K.; Watabe, M.; Nakaki, T. *J. Pharmacol. Sci.* **2008**, *108*, 227−238. (b) Forman, H. J.; Zhang, H.; Rinna, A. *Mol. Aspects Med.* **2009**, *30* (1−2), 1−12.
(16) Hayes, J. D.; Flanagan, J. U.; Jowsey, I. R. *Annu. Rev. Pharmacol. Toxicol.* **2004**, *45*, 51−88.
(17) Perdew, J. P.; Burke, K.; Ernzerhof, M. *Phys. Rev. Lett.* **1996**, *77*, 3865−3868.
(18) Allen, F. *Acta Crystallogr., Sect. B* **2002**, *58*, 380−388.
(19) Gorbitz, C. H. *Acta Chem. Scand., Ser. B* **1987**, *41*, 362−366.
(20) We used the pseudopotentials X.pbe-tm-gipaw.UPF (X = H, C, N, O, S) taken from: *QUANTUMESPRESSO*. www.quantum-espresso.org (2012).
(21) Sakellariou, D.; Lesage, A.; Hodgkinson, P.; Emsley, L. *Chem. Phys. Lett.* **2000**, *319*, 253−260.
(22) Paul, S.; Thakur, R. S.; Goswami, M.; Sauerwein, A. C.; Mamone, S.; Concistre, M.; Forster, H.; Levitt, M. H.; Madhu, P. K. *J. Magn. Reson.* **2009**, *197*, 14−19.
(23) Zhao, X.; Hoffbauer, W.; Schmedt auf der Gunne, J.; Levitt, M. H. *Solid State Nucl. Magn. Reson.* **2004**, *26*, 57−64.
(24) Fung, B. M.; Khitrin, A. K.; Ermolaev, K. *J. Magn. Reson.* **2000**, *142*, 97−101.
(25) Brinkmann, A.; Kentgens, A. P. M. *J. Am. Chem. Soc.* **2006**, *128*, 14758−14759.
(26) (a) Harris, R. K.; Olivieri, A. C. *Prog. Nucl. Magn. Reson. Spectrosc.* **1992**, *24*, 435−456. (b) Olivieri, A. C. *J. Magn. Reson.* **1989**, *81*, 201−205. (c) Olivieri, A. C.; Frydman, L.; Diaz, L. E. *J. Magn. Reson.* **1987**, *75*, 50−62.
(27) (a) Blinc, R.; Mali, M.; Osredkar, R.; Prelesnik, A.; Seliger, J.; Zupancic, I. *J. Chem. Phys.* **1972**, *57*, 5087−5093. (b) Giavani, T.; Bildsoe, H.; Skibsted, J.; Jakobsen, H. J. *J. Magn. Reson.* **2004**, *166*, 262−272.
(28) Webber, A. L.; Emsley, L.; Claramunt, R. M.; Brown, S. P. *J. Phys. Chem. A* **2010**, *114*, 10435−10442.
(29) (a) Gan, Z. *J. Am. Chem. Soc.* **2006**, *128*, 6040−6041. (b) Tatton, A. S.; Pham, T. N.; Vogt, F. G.; Iuga, D.; Edwards, A. J.; Brown, S. P. *Cryst. Eng. Comm.* **2012**, *14*, 2654−2659.
(30) (a) Hansen, M. R.; Graf, R.; Sekharan, S.; Sebastiani, D. *J. Am. Chem. Soc.* **2009**, *131*, 5251−5256. (b) Tasios, N.; Grigoriadis, C.; Hansen, M. R.; Wonneberger, H.; Li, C.; Spiess, H. W.; Mullen, K.; Floudas, G. *J. Am. Chem. Soc.* **2010**, *132*, 7478−7487. (c) Schnell, I. *Prog. Nucl. Magn. Reson. Spectrosc.* **2004**, *45* (1−2), 145−207. (d) Hodgkinson, P. *Annu. Rep. NMR Spectrosc.* **2011**, *72*, 185−223. (e) Brown, S. P. *Solid State Nucl. Magn. Reson.* **2012**, *41*, 1−27.
(31) Brown, S. P.; Lesage, A.; Elena, B.; Emsley, L. *J. Am. Chem. Soc.* **2004**, *126*, 13230−13231.
(32) Brown, S. P. *Macromol. Rapid Commun.* **2009**, *30* (9−10), 688−716.